

Original Research

Deguelin and Paclitaxel Loaded PEG-PCL Nano-Micelles for Suppressing the Proliferation and Inducing Apoptosis of Breast Cancer Cells

Yali Wang^{1,2}, Yang Lan^{1,2}, Liang Wu^{1,2}, Shijin Zhang^{1,2}, Qiang Su^{1,2}, Qin Yang^{1,2,*}¹Department of Pharmacy, Nanchong Central Hospital, The Second Clinical Medical College, North Sichuan Medical College, 637000 Nanchong, Sichuan, China²Nanchong Key Laboratory of Individualized Drug Therapy, 637000 Nanchong, Sichuan, China*Correspondence: qinyang201@163.com (Qin Yang)

Academic Editor: Taeg Kyu Kwon

Submitted: 16 May 2023 Revised: 3 September 2023 Accepted: 24 September 2023 Published: 23 February 2024

Abstract

Background: Deguelin (DGL) is a natural flavonoid reported to exhibit antitumor effects in breast cancer (BC). PEG-PCL (Polyethylene Glycol- Polycaprolactone), as polymeric micelles, has biodegradability and biocompatibility. The aim of this study was to investigate whether the nanoparticulate delivery system, PEG-PCL could improve the bioavailability of DGL for suppressing proliferation of BC cells. **Methods:** PEG-PCL polymers were first prepared by ring-opening polymerization, and DGL and paclitaxel (PTX)-loaded PEG-PCL nano-micelles were formulated via the film dispersion method. The composition and molecular weight of PEG-PCL were analyzed by nuclear magnetic resonance and fourier Transform infrared spectroscopy (FTIR) spectra. Particle size, surface potential and hemolytic activity of micelles were assessed by dynamic light scattering, transmission electron microscopy and hemolysis assay, respectively. Then proliferation and apoptosis of MDA-MB-231 and MDA-MB-468 cells were tested with Edu staining, CCK-8, TUNEL staining, and Flow cytometer. Caspase 3 expression was also assessed by Western blot. **Results:** Our results first indicated that PEG₂₀₀₀-PCL₂₀₀₀ was successfully synthesized. DGL and PTX-loaded PEG-PCL nano-micelles were rounded in shape with a particle size of 35.78 ± 0.35 nm and a surface potential of 2.84 ± 0.27 mV. The micelles had minimal hemolytic activity. Besides, we proved that DGL and PTX-loaded PEG-PCL nano-micelles could suppress proliferation and induce apoptosis in BC cells. The DGL and PTX-loaded PEG-PCL nano-micelles constructed in this study had a prominent inhibitory role on proliferation and a remarkable promotional role on apoptosis in BC cells. **Conclusions:** This study proposes that nano-micelles formed by PEG-PCL can enhance the cytotoxicity of Paclitaxel against breast cancer cells, and concurrently, the loading of Deguelin may further inhibit cell proliferation. This presents a potential for the development of a novel therapeutic strategy.

Keywords: PEG-PCL; deguelin; paclitaxel; breast cancer; apoptosis; proliferation

1. Introduction

Breast cancer (BC) is the most frequently occurring malignancy in women with a high lethality rate [1]. The causes of BC are complex and can be related to breast density, family history, and lifestyle habits, with genetic factors accounting for 5–10% [2]. For instance, individuals with mutations in the *BRCA1* or *BRCA2* genes have a higher likelihood of developing BC [3]. So far, the primary treatments for BC include surgical intervention, radiotherapy, chemotherapy, and endocrine therapy [4]. Endocrine therapy depends on the tumor subtype of breast cancer (HER, PR, ER), while for triple-negative breast cancer, only radiotherapy, chemotherapy, and surgical methods can be relied upon [5]. Paclitaxel, a first-line drug for breast cancer, exerts a broad killing effect on BC cells. However, the delivery of the drug relates to its killing efficiency and directly affects the therapeutic outcome [6]. Given the above circumstances, there is an urgent need to develop a method that can treat paclitaxel (PTX)-resistant breast cancer at lower doses, with little or no damage to the patient's normal tissues.

Systemic therapies are inefficient with a high recurrence rate due to systemic toxicity and drug resistance [7]. Additionally, Paclitaxel (PTX) - a commonly used first-line chemotherapeutic agent for BC treatment, effectively controls the disease and prolongs patient survival. However, the PTX-resistant BC will be developed after continuous chemotherapy with PTX [8]. Given this situation, there is an urgent need to develop a treatment method for PTX-resistant BC that uses lower doses and causes little to no damage to a patient's normal tissues.

Deguelin (DGL) is a flavonoid extracted from the legume family, having the chemical formula $C_{23}H_{22}O_6$ [9]. Growing evidence suggested that DGL has multiple pharmacological activities, including anti-inflammatory, antioxidant and antitumor effects [9,10]. Beyond preventing angiogenesis to exert potent anticancer activity [11]. DGL has chemotherapeutic and chemopreventive roles on several types of cancers [11,12]. Additionally, the action of DGL is highly specific and its main targets are tumor cells and precancerous cells, while it has little effect on normal cells [13]. Currently, DGL is also of great interest due to



its anticancer properties with high efficacy, and low toxicity [10]. Among the powerful anti-cancer mechanisms of DGL, induction of apoptosis and suppression of proliferation are the main means [14]. Additionally, combining DGL with other chemotherapy drugs can also enhance the efficacy and reverse the resistance of cancer cells caused by chemotherapy [15]. Several studies have also underscored the significance of DGL in BC treatment [16–18]. For example, DGL could block the growth of BC cells by Wnt pathway [19]; DGL could selectively induce the apoptosis of BC cells [17]; DGL could suppress the metastasis of BC cells [20]; and DGL could inhibit PI3K/AKT/MAP pathway in BC cells [18]. Nevertheless, the low bioavailability of entities like DGL limits their clinical application [21]. PEG-PCL (Polyethylene Glycol- Polycaprolactone) NDS (nanoparticulate delivery systems) can be effective over a longer period of time by releasing the drug slowly.

Clinically, numerous efficacious drugs are not broadly used due to limitations of their physicochemical properties, leading to low bioavailability and high toxic side effects. There are reports suggesting that the development of NDS (nanoparticulate delivery systems) with biocompatible polymers can enhance the physicochemical properties of drugs [22]. NDS, as a novel field of nanotechnology application, has great potential in the field of tumor therapy [23]. The encapsulated drugs in NDS gain protection from premature degradation, thereby improving their stability [24]. Furthermore, enhanced permeability and retention (EPR) in solid tumors enable NDS to aggregate in tumor tissues, thereby enhancing the bioavailability of drugs [25]. Among them, PEG-PCL is biocompatible and can self-assemble to form polymeric nanocarriers with different structures [26]. This nanopolymer can solve the problems of poor water solubility and stability of the drug, reducing toxicity and increasing efficacy through slow release and EPR effects [27]. However, it hasn't been reported whether NDS (DGL-PTX-PEG-PCL) can halt the malignant progression of BC cells.

In summary, we developed PEG-PCL nanoparticles laden with DGL and PTX (DGL-PTX-PEG-PCL), and evaluated their particle size, surface potential, and hemolytic properties. Additionally, we examined the nanomicelles' impact on BC cell proliferation and apoptosis. Therefore, our current study laid the foundation for the *in vivo* pharmacodynamic study of DGL-PTX-PEG-PCL and provide a reference for the study of novel nano formulations of DGL and similar drugs.

2. Materials and Methods

2.1 Synthesis of PEG-PCL

Dodecanol (1.86 g, 10 mmol) was dried under vacuum at 50 °C for 5 h, followed by the addition of Sn (Oct)₂ and continued drying for 0.5 h. Then the dried ϵ -caprolactone (16.8 g, 15 mmol) was added and reacted at 105 °C for 24 h. After cooling, the reaction system was added with a small

amount of ethanol and dissolved in tetrahydrofuran. After precipitation in cold diethyl ether, the mixture was filtered and dried to obtain PCL-OH.

PCL-OH (6.0 g, 3 mmol) was dried under vacuum at 50 °C for 8 h, dissolved in 30 mL of trichloromethane, added with succinic anhydride (1.5 g, 15 mmol) at 70 °C for 48 h. After cooling, the precipitated succinic anhydride was removed by filtration, precipitated in cold ethanol, and dried by filtration to obtain PCL-COOH.

PCL-COOH (4.0 g, 2 mmol) was dried under vacuum for 5 h, dissolved in 20 mL dichloromethane, and supplemented with NHS (0.46 g, 4 mmol). The mixture was placed in an ice bath, after which, DCC (0.82 g, 4 mmol) was added, and the reaction continued with stirring for 24 h. Then the insoluble DCU was removed by filtration, and the filtrate was precipitated in cold ether. After filtration, the filtrate was washed once with ether and isopropanol, and dried to obtain PCL-NHS.

PEG (2.0 g, 1 mmol) was dried under vacuum at 90 °C for 8 h. After dissolving in 10 mL dimethyl sulfoxide (DMSO), PEG was added with 10 mL THF solution containing PCL-NHS (2.0 g, 1 mmol) and stirred for 24 h. The resulting solution was dialyzed in deionized water for 3 d to obtain the PEG-PCL. In this study, the PEG-PCL micelle materials were provided by Tanshui Technology Co., Ltd. (Guangzhou, China) as a technical service.

2.2 Characterization Detection of PEG-PCL

For ¹H NMR, the polymers were dissolved with deuterated chloroform, and the chemical shifts of each proton were determined on a Varian Mercury-Plus 400 instrument. Tetramethylsilane (TMS) was used as an internal standard. Solid samples were mixed with dry KBr powder, finely ground and pressed. IR test was conducted on an infrared spectrometer (Nicolet/Nexus 670) with the wavelength of 400–4000 cm⁻¹.

2.3 Preparation of DGL and PTX-loaded PEG-PCL

40 mg of PEG-PCL was dissolved in 2 mL of chloroform, to which 20 mL of ultrapure water was slowly added under ultrasonication, using a sonicator (Scientz, Ningbo, China), to form an emulsion. The aqueous phase solution of blank micelles was obtained by rotary evaporator to remove chloroform at 30 °C. The blank micelles were concentrated by ultrafiltration three times, aggregates were removed by filtration using a 0.22 μ m filter, and the product was stored at 4 °C. 3 mg PTX and 3 mg DGL (Selleck Chemicals, USA) were dissolved in 1 mL DMSO, which were added to 1.5 mL chloroform containing 40 mg polymer. Then 20 mL ultrapure water was added slowly under ultrasonication to form an emulsion, and the chloroform was removed by rotary evaporation. The product was added to a dialysis bag with a molecular retention capacity of 14000 Da for more than 24 h. After ultrafiltration concentration and filtration, the product was stored at 4 °C.

2.4 Dynamic Light Scattering (DLS)

The micelle particle size and surface potential were measured using a Brookhaven Instruments BI-200 SM DLS system at 25 °C. The scattered light was detected at 90° and collected on an automatic accelerator. The surface potential was tested with a micro-detection device (Brookhaven Instruments, BI Zetaplus), as Zhong *et al.* [28] described.

2.5 Transmission Electron Microscopy (TEM)

10 µL of DGL and PTX-loaded PEG-PCL micelles (0.5 mg/mL) were deposited onto TEM copper grids and then placed in a desiccator for 8 h. The samples were stained with a 2% solution of acetyldioxymethylcellulose for 1 min, and the excess solution was then blotted with filter paper. After drying overnight at 60 °C, the samples were examined under a Transmission Electron Microscope (TEM) with an operating voltage of 120 kV.

2.6 Hemolysis Assay

Blood samples were centrifuged at 1500 × g for 10 min to obtain erythrocytes. 300 µL of erythrocyte suspension was added to 1.5 mL deionized water (positive control) and 1.5 mL solution containing 0 ppm, 100 ppm, 200 ppm, 400 ppm, and 800 ppm PEG-PCL micelles, respectively. After being left to stand for 3 hours at 37 °C, the absorbance of the supernatant was tested at 541 nm using a UV spectrophotometer to analyze the release of hemoglobin. The percentage of hemolysis for each sample was calculated by the formula $(A_{\text{sample}} - A_{\text{negative}}) / (A_{\text{positive}} - A_{\text{negative}})$. A_{sample} is the absorbance in the sample group, and A_{positive} is the absorbance in the positive group, and A_{negative} is the absorbance in the negative group. Solution without micelles (0 ppm) was set as a control solution in this experiment.

2.7 Cell Culture and Treatment

Both MDA-MB-231 and MDA-MB-468 cells were all purchased from the ATCC and then induced then into PTX-resistant cells. Both types of cells were grown in L-15 medium (GIBCO, Thermo Fisher Scientific, MA, USA) including 10% fetal bovine serum (Gibco, USA) at 37 °C with 5% CO₂. The breast cancer cells used in our experiments were meticulously cultured under stringent conditions. They underwent rigorous mycoplasma testing to ensure their contamination-free status. To establish PTX-resistant cell lines, breast cancer cells were subjected to a treatment involving a gradual escalation in the concentrations of PTX [29]. For non-nanoparticle encapsulated PTX and/or DGL, DMSO (0.1%) was used for dissolution to treat cells. In this study, the concentrations (or equivalent concentrations) of PTX and DGL used were 50 ng/mL and 60 ng/mL, respectively. All cell lines were authenticated shortly before use by the PCR technique, carried out by Zhongqiaoxinzhou Biotech (Shanghai, China).

2.8 EdU Staining

EdU solution (Solarbio, Beijing, China) was diluted with culture medium to prepare 50 µM EdU medium. MDA-MB-231 and MDA-MB-468 cells (1×10^4 cells) were collected, washed, and counted. Then the cells were equally inoculated in a 96-well plate and treated in the light of experimental purpose. The treated BC cells were supplemented with 100 µL 50µM EdU medium for 2 h. After washing, cells were fixed by 50 µL 4% paraformaldehyde for 30 min and permeabilized by 0.5% Triton X-100. Subsequently, the cells were exposed to 50 µL of 2 mg/mL glycine for 5 min. the results were obtained with a fluorescence microscopy (Excitation wavelength: 555 nm; Emission wavelength: 565 nm).

2.9 CCK-8

Each group of cells were digested using trypsin (0.25%) and suspended in culture medium. After that, cells in each well were addressed with 10 µL of CCK-8 (Dojindo, Kumamoto, Japan) and incubated for another 3 h. The OD value was tested using a microplate reader at 450 nm.

2.10 TUNEL Staining

The cells of each group were fixed using 4% paraformaldehyde for 15 min after removing the culture medium, then incubated with 0.1% TritonX-100 in ice bath for 2 min. After washing, the cells were exposed to 0.3% hydrogen peroxide in methanol for 20 min. Subsequently, appropriate TUNEL solution (Beyotime, Shanghai, China) was added to each well of cells and incubated for 1 h at 37 °C protected from light. After washing, the cells were treated with TUNEL working solution for 10 min, ethanol (dehydration) for 2 min, and xylene (transparency) for 2 times. After sealing, TUNEL positive cells were observed under a fluorescence microscope.

2.11 Flow Cytometer

Annexin-FITC/PI apoptosis kit (BD Biosciences, NJ, USA) was utilized for apoptosis analysis. After processing, each group of cells (5×10^5 , 200 µL) was collected and treated with AnnexinV-FITC (5 µL) and PI (5 µL) for 30 min in the dark. Then the cells were washed using 190 µL binding buffer, centrifuged, and resuspended with phosphate buffered saline (PBS). Flow cytometry (FACSCalibur; BD Biosciences, NJ, USA) was used to analyze cell apoptosis.

2.12 Western Blot

BC cells from each group were added with 100 µL protein lysate. After ice bath and centrifugation, the supernatant was harvested. Protein concentration was confirmed by applying BCA kit (Beyotime, Shanghai, China). 20 µg of protein was mixed with 5× loading buffer and denatured. Then groups of samples were applied for SDS-PAGE electrophoresis, and electrotransferred onto PVDF membranes. After incubation with 5% skim milk powder for 2 h, the

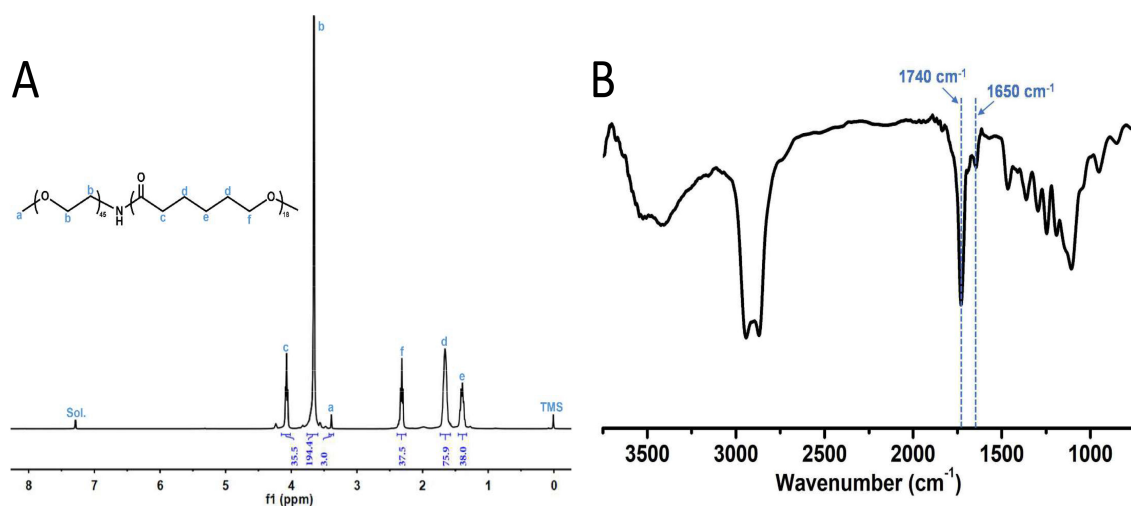


Fig. 1. nuclear magnetic resonance (NMR) spectrum and fourier transform infra-red (FTIR) spectra of PEG-PCL. (A) ^1H NMR spectra (CDCl_3 , 400MHz) of PEG-PCL. The proton characteristic chemical shifts are attributed to $\delta 3.38\text{ppm}$ $\text{CH}_3(\text{OCH}_2\text{CH}_2)-$, a; $\delta 3.65\text{ppm}$ $\text{CH}_3(\text{OCH}_2\text{CH}_2)-$, b; $\delta 4.05\text{ppm}$ $-\text{NH}-(\text{COCH}_2\text{CH}_2\text{CH}_2\text{CH}_2\text{CH}_2\text{O}) \text{CH}_3$, c; $\delta 1.66\text{ppm}$ $-\text{NH}-(\text{COCH}_2\text{CH}_2\text{CH}_2\text{CH}_2\text{CH}_2\text{O}) \text{CH}_3$, d; $\delta 1.41\text{ppm}$ $-\text{NH}-(\text{COCH}_2\text{CH}_2\text{CH}_2\text{CH}_2\text{CH}_2\text{O}) \text{CH}_3$, e; $\delta 2.33\text{ppm}$ $-\text{NH}-(\text{COCH}_2\text{CH}_2\text{CH}_2\text{CH}_2\text{CH}_2\text{O}) \text{CH}_3$, f. The number of hydrogen atoms in the repeating unit of the PEG backbone was 194, based on the methoxy peak of PEG. The molecular weight of PEG was calculated to be 2138 Da based on the molecular weight of each repeating unit ($M_w = 44$ Da). (B) FTIR spectra of PEG-PCL. NMR, nuclear magnetic resonance; FTIR, fourier transform infra-red; PEG-PCL, polyethylene glycol- polycaprolactone.

membranes were treated with the diluted primary antibodies including Caspase 3 (Abcam, 1:500) and GAPDH (Abcam, 1:8000) overnight at 4°C , and the secondary antibody (Abcam, 1:10,000) for 2 h. After treatment with PierceTM ECL substrate (Thermo Fisher Scientific, MA, USA), the blots were obtained using an ECL system (Thermo Fisher Scientific, MA, USA). A GAPDH was used as an internal reference.

2.13 Statistical Analysis

All experiments were independently repeated 3 times and the data were denoted as mean \pm SD. Data were analyzed using SPSS 23.0 software (IBM Inc., Chicago, IL, USA). A one-way ANOVA, followed by a Tukey's test, was used to analyze the difference between groups. $p < 0.05$ was regarded as a significant difference.

3. Results

3.1 NMR Spectrum and FTIR Spectra of PEG-PCL

The structure of PEG-PCL was confirmed by ^1H NMR (nuclear magnetic resonance) (Fig. 1A). The molecular weight of PCL was calculated as 2054 Da in the same way, which is consistent with our designed molecular weight of PEG2000-PC2000. Therefore, results showed that PEG-PCL has been successfully synthesized. The characterization of FTIR (fourier transform infra-red) spectra showed that 1740 cm^{-1} is the $\text{C}=\text{O}$ absorption peak in the ester bond, and 1650 cm^{-1} is the $\text{C}=\text{O}$ absorption peak in the amide bond (Fig. 1B). These characteristic peaks further demonstrate the successful synthesis of PEG-PCL.

3.2 Particle Size and Morphology Characterization of DGL and PTX-Loaded PEG-PCL Nano-Micelle

Next, the data of DLS signified that the average particle size and surface potential of micelles formed by blank carriers were 30.86 ± 2.1 nm and -3.55 ± 0.27 mV, respectively. The average particle size and surface potential of micelles loaded with DGL and PTX were 35.78 ± 0.35 nm and -2.84 ± 0.27 mV. Compared with the control micelles, the particle size of micelle loaded with DGL and PTX increased and the potential was slightly reduced (Fig. 2A). Besides, TEM was applied to determine the morphological structure of nanomicelles loaded with DGL and PTX at pH 7.4. The results denoted that the nanomicelles exhibited a uniform spherical structure with a particle size around 30 nm, which was similar to the DLS results (Fig. 2B). In this manner, we determined the physicochemical properties of DGL and PTX-loaded PEG-PCL.

3.3 Loading Capacities, Critical Micelle Concentration, Serum Stability Test and Hemolysis Caused by Micelles at Different Concentrations

Specifically, the acetonitrile solution of PTX showed the maximum absorption at 227 nm, while the DMSO solution of DGL showed the maximum absorption at 272 nm. The standard curve concerning concentration for PTX was: $A = 0.02951c + 0.00173$, $R^2 = 0.99627$; whereas, for DGL with respect to concentration, it was: $A = 0.05549c - 0.02276$, $R^2 = 0.99829$. Having obtained the absorbance of PTX and DGL in the micelles, their loading capacities were calculated to be $5.3 \pm 0.17\%$ and $6.1 \pm 0.21\%$, re-

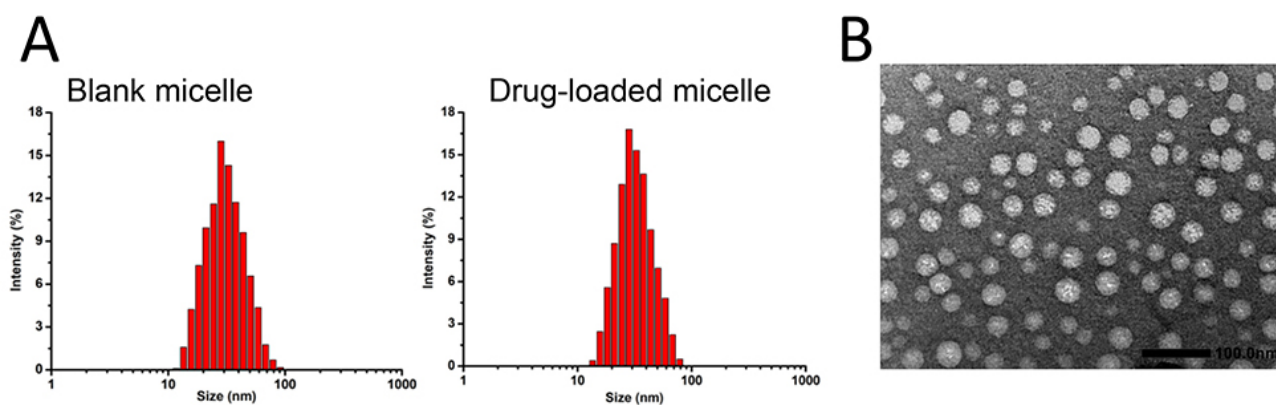


Fig. 2. Particle size and morphology characterization of deguelin (DGL) and paclitaxel (PTX)-loaded polyethylene glycol-polycaprolactone (PEG-PCL) nano-micelle. (A) Particle sizes of blank micelle (left) and drug-loaded micelle (right) through dynamic light scattering assay. (B) Drug-loaded micelles were observed using TEM with uranyl acetate. DGL, deguelin.

spectively, based on the standard curves (Supplementary Fig. 1). Using the pyrene fluorescence probe method, the critical micelle concentration (CMC) of the sample was measured. The results indicated that the CMC for PEG_{2k}-PCL_{2k} was 19.95 $\mu\text{g/mL}$ (4.99×10^{-6} mol/L), as shown in Supplementary Fig. 2. Serum Stability Test showed that drug-loaded micelles displayed excellent size stability in the PBS solution with 10% FBS, maintaining a particle size of around 35 nm over a week (Supplementary Fig. 3).

Crucially, we further validated the blood biocompatibility of the micelles. Once hemolysis occurs, the hemoglobin in the red blood cells will be released into the solution. The redness of this solution, indicating hemolytic activity, can be estimated by measuring the UV absorbance of the supernatant at 541 nm. As represented in Fig. 3, there was no significant hemolysis in micelles at the experimental concentrations (100–800 ppm). Even at a concentration of 800 ppm, only about 4% hemolysis occurred in micelles at 3 h exposure time. Therefore, the hemolytic activity of micelles was negligible.

3.4 DGL and PTX-Loaded PEG-PCL Nano-Micelles Suppresses BC Cell Proliferation

Subsequently, we validated the impact of DGL and PTX-loaded PEG-PCL nano-micelles on the proliferation of BC cells. MDA-MB-231 and MDA-MB-468 cells were treated with PEG-PCL, PTX, DGL, PTX+DGL, DGL/PEG-PCL, PTX/PEG-PCL, and DGL-PTX/PEG-PCL. EdU staining results displayed that PEG-PCL, PTX, and DGL treatment alone did not significantly affect the proliferative activity of the BC cells; Four combined treatments including PTX+DGL, DGL/PEG-PCL, PTX/PEG-PCL, and DGL-PTX/PEG-PCL could observably reduce BC cell proliferation activity, especially DGL-PTX/PEG-PCL (Fig. 4A). Similarly, CCK-8 data showed that treatment of PEG-PCL, PTX, and DGL alone also failed to induce changes in BC cell viability; Combined treatments (PTX+DGL, DGL/PEG-PCL, PTX/PEG-PCL, and DGL-

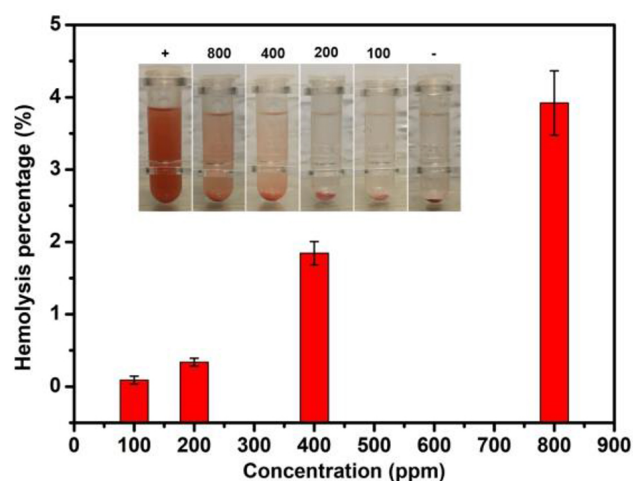


Fig. 3. Hemolysis caused by micelles at different concentrations. Hemolysis assay was conducted after processing with different concentrations of micelles. Deionized water was served as a positive control (+) and phosphate buffered saline (PBS) as a negative control (-). PBS, phosphate buffered saline.

PTX/PEG-PCL) also could markedly restrain BC cell proliferation viability, and this suppression effect was strongest in the DGL-PTX/PEG-PCL group (Fig. 4B). Overall, these data suggest that DGL and PTX-loaded PEG-PCL nano-micelles can cause a remarkable reduction in BC cell proliferation.

3.5 DGL and PTX-Loaded PEG-PCL Nano-Micelles Induces BC Cell Apoptosis

We also further confirmed the changes in apoptosis of BC cells after treatment with DGL and PTX-loaded PEG-PCL nano-micelles. Data from TUNEL indicated that PEG-PCL, PTX, DGL alone did not lead to prominent changes in the apoptotic capacity of BC cells; relative to the control (DMSO) group, the apoptotic capacity of BC cells was significantly increased in PTX+DGL, DGL/PEG-PCL, PTX/PEG-PCL, and DGL-PTX/PEG-PCL groups, espe-

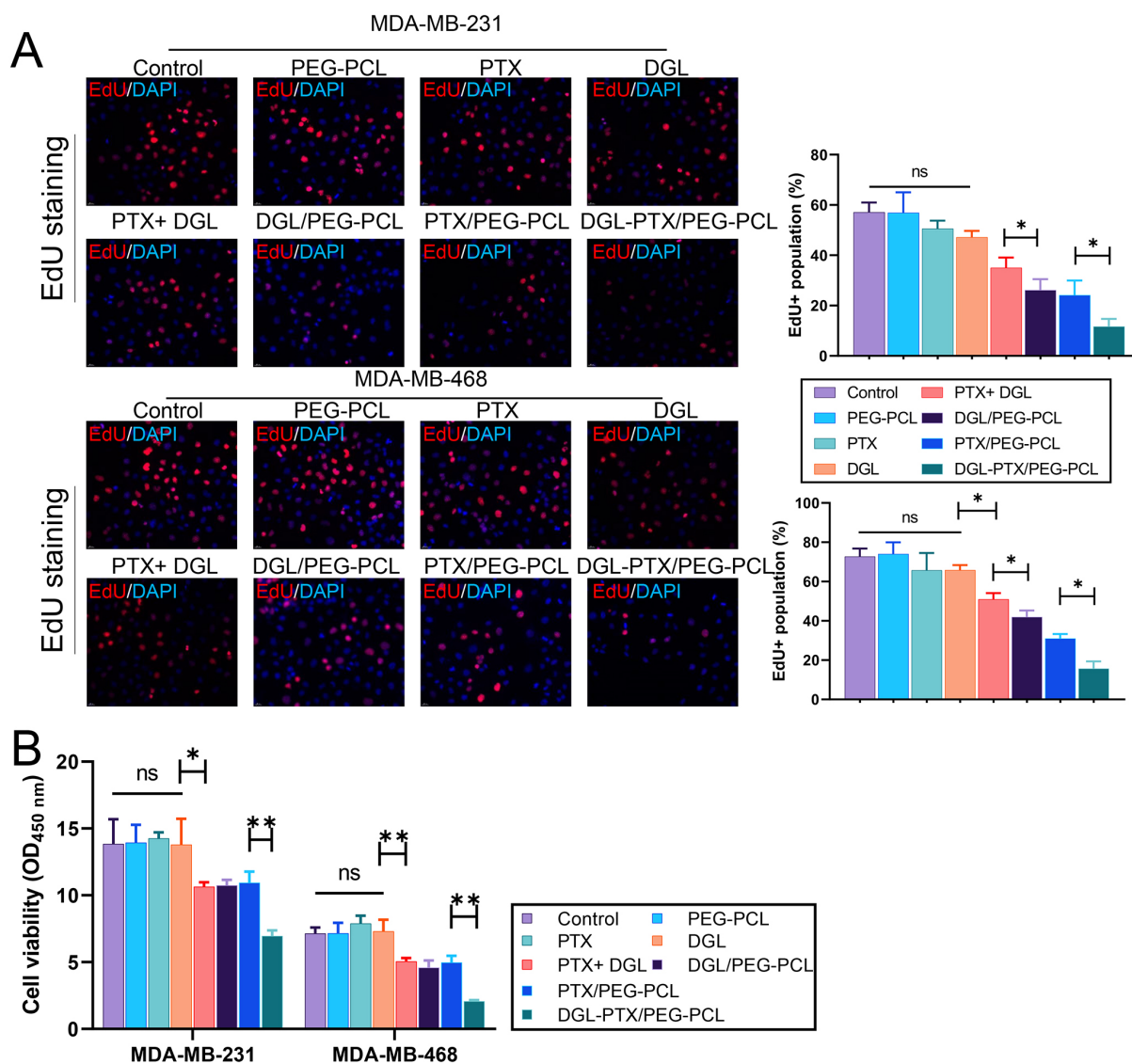


Fig. 4. DGL and PTX-loaded PEG-PCL nano-micelles suppresses the proliferation of breast cancer (BC) cells. MDA-MB-231 and MDA-MB-468 cells were dealt with DMSO, PEG-PCL, PTX, DGL, PTX+DGL, DGL/PEG-PCL, PTX/PEG-PCL, and DGL-PTX/PEG-PCL, respectively. (A) Cell proliferative activity was confirmed with Edu staining. Magnification, 200 \times . (B) Cell viability was monitored through CCK-8. NS means no significance; * means $p < 0.05$; ** means $p < 0.01$.

cially in DGL-PTX/PEG-PCL group (Fig. 5A). Flow cytometer data also indicated that PTX+DGL, DGL/PEG-PCL, PTX/PEG-PCL, and DGL-PTX/PEG-PCL could dramatically induce BC cell apoptosis, and relative to other groups, DGL and PTX-loaded PEG-PCL nano-micelles (DGL-PTX/PEG-PCL) had the strongest induction of apoptosis in BC cells (Fig. 5B). Additionally, western blot data showed that Caspase 3 expression was notably upregulated in PTX+DGL, DGL/PEG-PCL, PTX/PEG-PCL, and DGL-PTX/PEG-PCL groups versus that in DMSO group; and the degree of upregulation of Caspase 3 expression was most significant in DGL-PTX/PEG-PCL group (Fig. 5C). Thus, we testified that DGL and PTX-loaded PEG-PCL nano-micelles can result in a noteworthy elevation in apoptotic capacity of BC cells.

4. Discussion

Breast cancer (BC) is characterized by its aggressive progression and high mortality rate. The killing effect of drugs on tumor cells is fundamental to anti-tumor therapy. PTX is a taxane compound with strong anti-malignant effects [30]. PTX, as a chemotherapeutic agent, has been widely utilized in malignant tumors, especially BC [8,31]. Moreover, drug resistance is one of the key reasons for therapeutic failure in BC patients [31]. The main factors causing PTX resistance mainly cover gene mutations, ABC transporters, and side effects, etc [8]. Currently, the carrier of PTX is mostly polyoxyethylated castor oil, which can lead to allergic reactions [32]. Literature suggests, we discovered that PTX nanoparticles for BC-targeted therapy offer a stable and effective therapeutic intervention [33].

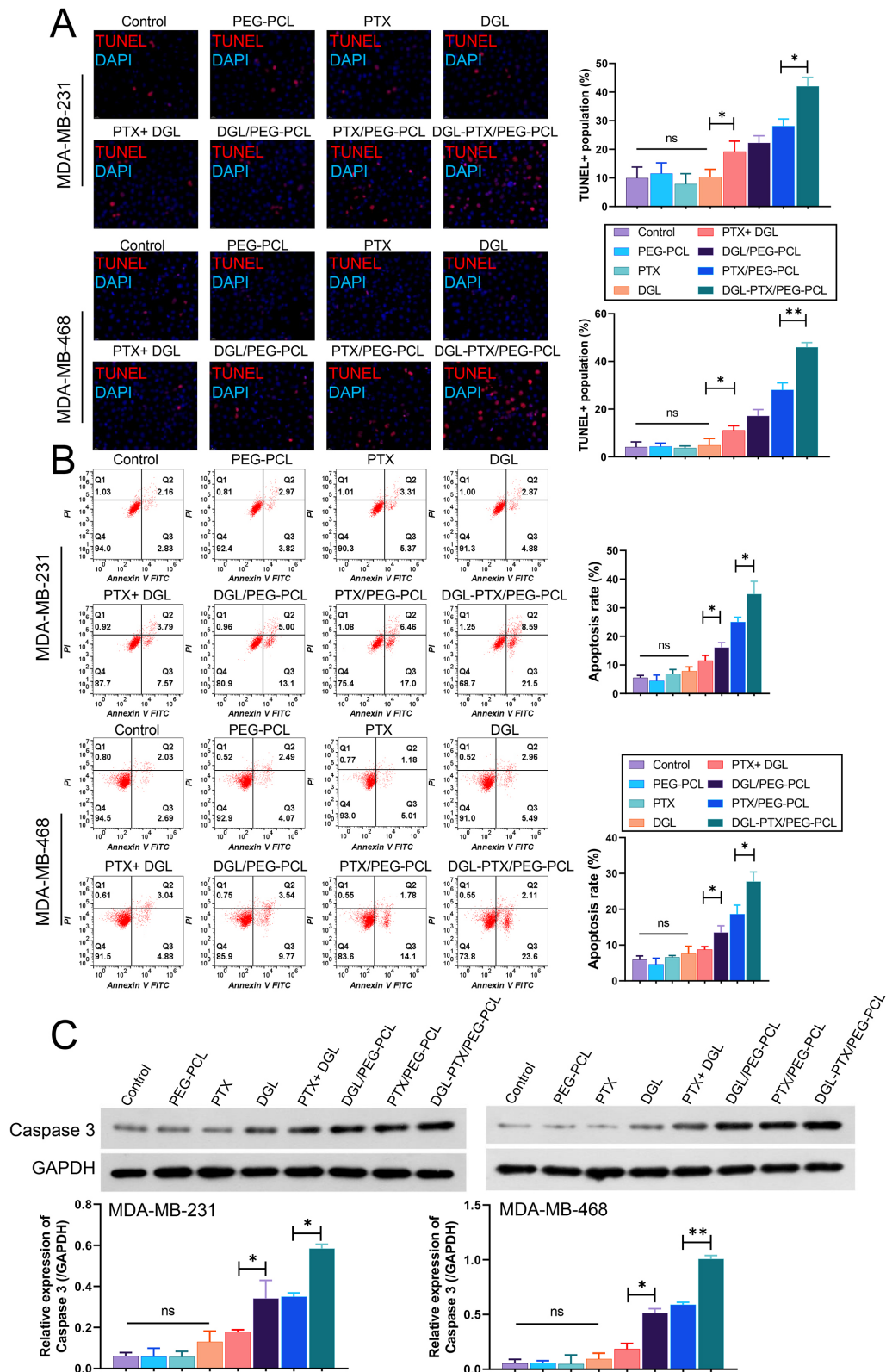


Fig. 5. DGL and PTX-loaded PEG-PCL nano-micelles induces the apoptosis of BC cells. MDA-MB-231 and MDA-MB-468 cells were also processed with dimethyl sulfoxide (DMSO), PEG-PCL, PTX, DGL, PTX+DGL, DGL/PEG-PCL, PTX/PEG-PCL, and DGL-PTX/PEG-PCL, respectively. (A) Cell apoptosis was determined with TUNEL staining. Magnification, 200 \times . (B) Flow cytometer was utilized to monitor the role of DGL and PTX-loaded PEG-PCL nano-micelles on cell apoptosis. (C) Western blot exhibited the alteration of Caspase 3 expression in each group. NS means no significance; * means $p < 0.05$; ** means $p < 0.01$.

Currently, Nanodelivery systems have garnered significant attention in recent years for their potential in drug delivery, with nanoparticles, liposomes, and micelles being among the most prevalent. Nanoparticles, typically composed of natural or synthetic polymers, encapsulate drugs for sustained release [34]. Liposomes, vesicles formed from phospholipid bilayers, can encapsulate both hydrophilic and lipophilic drugs [35]. Micelles, self-assembled from amphiphilic molecules, stand out for their hydrophilic shell and lipophilic core, making them particularly adept at delivering lipophilic drugs [36]. This unique structure of micelles enhances drug solubility and stability, offering a promising avenue for targeted and efficient drug delivery. PEG-PCL copolymer exhibits biocompatibility and biodegradability, implying that they do not induce adverse side effects *in vivo* and can naturally degrade upon fulfilling their therapeutic purpose [37]. PEG-PCL micelles significantly enhance the solubility of pharmaceutical agents, particularly those inherently insoluble [38]. Furthermore, PEG-PCL micelles can be engineered to target specific cells or tissues, ensuring precise drug delivery [37]. In fact, multiple studies have utilized PEG-PCL as a carrier to construct drug delivery systems [26,39]. PEG-PCL polymer is synthesized by ring-opening polyaddition of caprolactone monomer at high temperature with stannous octanoate as catalyst and methoxy-polyethylene glycol as macroinitiator [40]. PEG is a hydrophilic segment and PCL is a hydrophobic segment [41]. The length and molar ratio of hydrophilic and hydrophobic segments can be controlled during the synthesis of PEG-PCL to produce polymers with different molecular weights and mass ratios of hydrophilic and hydrophobic segments [27]. *In vivo*, after the hydrolysis of PCL ester bonds, the long chains break and form small fragments, which are eventually metabolized and absorbed by the body [42]. It was also discovered that PCL had a mild inflammatory response for a short time after entering the body, which then disappeared, and that PCL had little influence on immune cell activity [43]. Overall, PCL and PEG are biocompatible materials. PEG is water-soluble, non-antigenic and immunogenic, and can evade recognition by the human macrophage system [44]. Studies have shown that drug-loaded PEG-PCL micelles can be applied in cancer therapies through drug delivery. For instance, ditelluride-loaded PEG-PCL can enhance cancer therapy [45]; Gambogic acid-loaded PEG-PCL can improve anti-tumor efficiency against gastric cancer [46]; docetaxel-loaded PEG-PCL can serve an effective anti-tumor agent against prostate cancer [47]; and doxorubicin-bridged PEG-PCL-PEG has an inhibitory effect on the BC progression [48]. Therefore, we suggested that the PEG-PCL micelles have a time-controlled release property *in vitro* and are expected to be a stable, effective, and safe vehicle in cancer chemotherapy. In our study, we also successfully synthesized PEG-PCL through ring-opening polymerization based on previous research [39].

Deguelin (DGL), an isoflavone, has been reported to have regulatory roles on cancer cell proliferation, growth, cell cycle distribution, and apoptosis [9]. DGL has a high safety profile and a promising application as a potential natural antitumor agent. Multiple studies also have reported that DGL can prevent the growth of BC cells [16,49], suggesting that DGL is effective in BC therapy. Additionally, DGL is a novel Akt inhibitor with strong anti-tumor effects [50,51]. Multiple studies revealed that Akt pathway is in connection with the PTX resistance of BC [52,53]. Furthermore, deguelin analogues can hinder the progression of PTX-resistant non-small cell lung cancer [54]. Therefore, we speculated that the combined application of DGL and PTX might have an obvious effect on BC therapy. To achieve a lower dosage, reverse drug resistance, and ensure high safety in BC therapy, we constructed an efficient NDS using PEG-PCL as a carrier to co-deliver DGL and PTX. Our results indicated that DGL and PTX-loaded PEG-PCL nano-micelles had stronger effects on cell proliferation inhibition and apoptosis induction in BC cells than DGL alone, PTX alone or DGL and PTX combination. Additionally, the BC inhibitory effects of DGL-loaded PEG-PCL or PTX-loaded PEG-PCL were not as potent as DGL and PTX-loaded PEG-PCL nano-micelles.

5. Conclusions

In summary, we enhanced the anti-BC properties of DGL and PTX and increased the drug's *in vitro* effectiveness through the construction of PEG-PCL nanoscale micelles (NSM). Future studies will explore the distribution and anti-tumor activity of DGL and PTX-loaded PEG-PCL nano-micelles *in vivo*.

Availability of Data and Materials

The datasets used and/or analyzed during the current study are available from the corresponding author on reasonable request.

Author Contributions

QY and YW designed the research study. YW and YL performed the research. LW, SZ and QS analyzed the data. YW and YL wrote the manuscript. All authors contributed to editorial changes in the manuscript. All authors read and approved the final manuscript. All authors have participated sufficiently in the work and agreed to be accountable for all aspects of the work.

Ethics Approval and Consent to Participate

Not applicable.

Acknowledgment

Not applicable.

Funding

This research was funded by Sichuan Scientific Research Subject on Traditional Chinese Medicine (2021MS196), North Sichuan Medical College Doctoral Research Project (CBY19-QD06).

Conflict of Interest

The authors declare no conflict of interest.

Supplementary Material

Supplementary material associated with this article can be found, in the online version, at <https://doi.org/10.31083/j.fbl2902090>.

References

- [1] Fahad Ullah M. Breast Cancer: Current Perspectives on the Disease Status. *Advances in Experimental Medicine and Biology*. 2019; 1152: 51–64.
- [2] Coughlin SS. Epidemiology of Breast Cancer in Women. *Advances in Experimental Medicine and Biology*. 2019; 1152: 9–29.
- [3] Narod SA, Salmena L. BRCA1 and BRCA2 mutations and breast cancer. *Discovery Medicine*. 2011; 12: 445–453.
- [4] Henson KE, McGale P, Darby SC, Parkin M, Wang Y, Taylor CW. Cardiac mortality after radiotherapy, chemotherapy and endocrine therapy for breast cancer: Cohort study of 2 million women from 57 cancer registries in 22 countries. *International Journal of Cancer*. 2020; 147: 1437–1449.
- [5] Won KA, Spruck C. Triple negative breast cancer therapy: Current and future perspectives (Review). *International Journal of Oncology*. 2020; 57: 1245–1261.
- [6] Kang YJ, Yoon CI, Yang YJ, Baek JM, Kim YS, Jeon YW, *et al*. A randomized controlled trial using surgical gloves to prevent chemotherapy-induced peripheral neuropathy by paclitaxel in breast cancer patients (AIUR trial). *BMC Cancer*. 2023; 23: 570.
- [7] Burstein HJ, Curigliano G, Thürlimann B, Weber WP, Poortmans P, Regan MM, *et al*. Customizing local and systemic therapies for women with early breast cancer: the St. Gallen International Consensus Guidelines for treatment of early breast cancer 2021. *Annals of Oncology: Official Journal of the European Society for Medical Oncology*. 2021; 32: 1216–1235.
- [8] Abu Samaan TM, Samec M, Liskova A, Kubatka P, Büsselberg D. Paclitaxel's Mechanistic and Clinical Effects on Breast Cancer. *Biomolecules*. 2019; 9: 789.
- [9] Lin ZY, Yun QZ, Wu L, Zhang TW, Yao TZ. Pharmacological basis and new insights of deguelin concerning its anticancer effects. *Pharmacological Research*. 2021; 174: 105935.
- [10] Tuli HS, Mittal S, Loka M, Aggarwal V, Aggarwal D, Masurkar A, *et al*. Deguelin targets multiple oncogenic signaling pathways to combat human malignancies. *Pharmacological Research*. 2021; 166: 105487.
- [11] Li M, Yu X, Li W, Liu T, Deng G, Liu W, *et al*. Deguelin suppresses angiogenesis in human hepatocellular carcinoma by targeting HGF-c-Met pathway. *Oncotarget*. 2017; 9: 152–166.
- [12] Gao F, Yu X, Li M, Zhou L, Liu W, Li W, *et al*. Deguelin suppresses non-small cell lung cancer by inhibiting EGFR signaling and promoting GSK3 β /FBW7-mediated Mcl-1 destabilization. *Cell Death & Disease*. 2020; 11: 143.
- [13] Wang Y, Ma W, Zheng W. Deguelin, a novel anti-tumorigenic agent targeting apoptosis, cell cycle arrest and anti-angiogenesis for cancer chemoprevention. *Molecular and Clinical Oncology*. 2013; 1: 215–219.
- [14] Lee H, Lee JH, Jung KH, Hong SS. Deguelin promotes apoptosis and inhibits angiogenesis of gastric cancer. *Oncology Reports*. 2010; 24: 957–963.
- [15] Wang A, Wang W, Chen Y, Ma F, Wei X, Bi Y. Deguelin induces PUMA-mediated apoptosis and promotes sensitivity of lung cancer cells (LCCs) to doxorubicin (Dox). *Molecular and Cellular Biochemistry*. 2018; 442: 177–186.
- [16] Nguyen CT, Thanh La M, Ann J, Nam G, Park HJ, Min Park J, *et al*. Discovery of a simplified deguelin analog as an HSP90 C-terminal inhibitor for HER2-positive breast cancer. *Bioorganic & Medicinal Chemistry Letters*. 2021; 45: 128134.
- [17] Peng XH, Karna P, O'Regan RM, Liu X, Naithani R, Moriarty RM, *et al*. Down-regulation of inhibitor of apoptosis proteins by deguelin selectively induces apoptosis in breast cancer cells. *Molecular Pharmacology*. 2007; 71: 101–111.
- [18] Wu W, Hai Y, Chen L, Liu RJ, Han YX, Li WH, *et al*. Deguelin-induced blockade of PI3K/protein kinase B/MAP kinase signaling in zebrafish and breast cancer cell lines is mediated by down-regulation of fibroblast growth factor receptor 4 activity. *Pharmacology Research & Perspectives*. 2016; 4: e00212.
- [19] Murillo G, Peng X, Torres KEO, Mehta RG. Deguelin inhibits growth of breast cancer cells by modulating the expression of key members of the Wnt signaling pathway. *Cancer Prevention Research (Philadelphia, Pa.)*. 2009; 2: 942–950.
- [20] Mehta RR, Katta H, Kalra A, Patel R, Gupta A, Alimirah F, *et al*. Efficacy and mechanism of action of Deguelin in suppressing metastasis of 4T1 cells. *Clinical & Experimental Metastasis*. 2013; 30: 855–866.
- [21] Men K, Liu W, Li L, Duan X, Wang P, Gou M, *et al*. Delivering instilled hydrophobic drug to the bladder by a cationic nanoparticle and thermo-sensitive hydrogel composite system. *Nanoscale*. 2012; 4: 6425–6433.
- [22] Chen H, Liu H, Liu L, Chen Y. Fabrication of subunit nanovaccines by physical interaction. *Science China. Technological Sciences*. 2022; 65: 989–999.
- [23] Muhamad N, Plengsuriyakarn T, Na-Bangchang K. Application of active targeting nanoparticle delivery system for chemotherapeutic drugs and traditional/herbal medicines in cancer therapy: a systematic review. *International Journal of Nanomedicine*. 2018; 13: 3921–3935.
- [24] de la Torre P, Pérez-Lorenzo MJ, Alcázar-Garrido Á, Flores AI. Cell-Based Nanoparticles Delivery Systems for Targeted Cancer Therapy: Lessons from Anti-Angiogenesis Treatments. *Molecules (Basel, Switzerland)*. 2020; 25: 715.
- [25] Kalyane D, Raval N, Maheshwari R, Tambe V, Kalia K, Tekade RK. Employment of enhanced permeability and retention effect (EPR): Nanoparticle-based precision tools for targeting of therapeutic and diagnostic agent in cancer. *Materials Science & Engineering. C, Materials for Biological Applications*. 2019; 98: 1252–1276.
- [26] Grossen P, Witzigmann D, Sieber S, Huwyler J. PEG-PCL-based nanomedicines: A biodegradable drug delivery system and its application. *Journal of Controlled Release: Official Journal of the Controlled Release Society*. 2017; 260: 46–60.
- [27] Deng H, Dong A, Song J, Chen X. Injectable thermosensitive hydrogel systems based on functional PEG/PCL block polymer for local drug delivery. *Journal of Controlled Release: Official Journal of the Controlled Release Society*. 2019; 297: 60–70.
- [28] Zhong H, Chen G, Li T, Huang J, Lin M, Li B, *et al*. Nanodrug Augmenting Antitumor Immunity for Enhanced TNBC Therapy via Pyroptosis and cGAS-STING Activation. *Nano Letters*. 2023; 23: 5083–5091.
- [29] Kong Z, Han Q, Zhu B, Wan L, Feng E. Circ_0069094 regulates malignant phenotype and paclitaxel resistance in breast cancer cells via targeting the miR-136-5p/YWHAZ axis. *Thoracic Cancer*. 2023; 14: 1831–1842.
- [30] Sharifi-Rad J, Quispe C, Patra JK, Singh YD, Panda MK, Das G, *et al*. Paclitaxel: Application in Modern Oncology and

Nanomedicine-Based Cancer Therapy. *Oxidative Medicine and Cellular Longevity*. 2021; 2021: 3687700.

- [31] Dan VM, Raveendran RS, Baby S. Resistance to Intervention: Paclitaxel in Breast Cancer. *Mini Reviews in Medicinal Chemistry*. 2021; 21: 1237–1268.
- [32] Lee S, Miyajima T, Sugawara-Narutaki A, Kato K, Nagata F. Development of paclitaxel-loaded poly(lactic acid)/hydroxyapatite core-shell nanoparticles as a stimuli-responsive drug delivery system. *Royal Society Open Science*. 2021; 8: 202030.
- [33] Nieto C, Vega MA, Martín Del Valle E. Nature-Inspired Nanoparticles as Paclitaxel Targeted Carrier for the Treatment of HER2-Positive Breast Cancer. *Cancers*. 2021; 13: 2526.
- [34] Gagliardi A, Giuliano E, Venkateswararao E, Fresta M, Bullotta S, Awasthi V, *et al.* Biodegradable Polymeric Nanoparticles for Drug Delivery to Solid Tumors. *Frontiers in Pharmacology*. 2021; 12: 601626.
- [35] Domiński A, Domińska M, Skonieczna M, Pastuch-Gawolek G, Kurcok P. Shell-Sheddable Micelles Based on Poly(ethylene glycol)-hydrazone-poly[R,S]-3-hydroxybutyrate Copolymer Loaded with 8-Hydroxyquinoline Glycoconjugates as a Dual Tumor-Targeting Drug Delivery System. *Pharmaceutics*. 2022; 14: 290.
- [36] Adeli F, Abbasi F, Babazadeh M, Davaran S. Thermo/pH dual-responsive micelles based on the host-guest interaction between benzimidazole-terminated graft copolymer and β -cyclodextrin-functionalized star block copolymer for smart drug delivery. *Journal of Nanobiotechnology*. 2022; 20: 91.
- [37] Behl A, Solanki S, Paswan SK, Datta TK, Saini AK, Saini RV, *et al.* Biodegradable PEG-PCL Nanoparticles for Co-delivery of MUC1 Inhibitor and Doxorubicin for the Confinement of Triple-Negative Breast Cancer. *Journal of Polymers and the Environment*. 2023; 31: 999–1018.
- [38] Patmayuni D, Sulaiman TNS, Zulkarnain AK, Shiyan S. Method Validation of Simvastatin in Pcl-Peg-Pcl Triblock Copolymer Micelles Using Uv-Vis Spectrophotometric for Solubility Enhancement Assay. *International Journal of Applied Pharmaceutics*. 2022; 14: 246–250.
- [39] Nosrati H, Barzegari P, Danafar H, Kheiri Manjili H. Biotin-functionalized copolymeric PEG-PCL micelles for *in vivo* tumour-targeted delivery of artemisinin. *Artificial Cells, Nanomedicine, and Biotechnology*. 2019; 47: 104–114.
- [40] Kuplennik N, Sosnik A. Enhanced Nanoencapsulation of Sepiapterin within PEG-PCL Nanoparticles by Complexation with Triacetyl-Beta Cyclodextrin. *Molecules (Basel, Switzerland)*. 2019; 24: 2715.
- [41] Park C, Yoo J, Lee D, Jang SY, Kwon S, Koo H. Chlorin e6-Loaded PEG-PCL Nanoemulsion for Photodynamic Therapy and *In Vivo* Drug Delivery. *International Journal of Molecular Sciences*. 2019; 20: 3958.
- [42] Lee HJ, Jeong B. ROS-Sensitive Degradable PEG-PCL-PEG Micellar Thermogel. *Small (Weinheim an Der Bergstrasse, Germany)*. 2020; 16: e1903045.
- [43] Gou M, Wei X, Men K, Wang B, Luo F, Zhao X, *et al.* PCL/PEG copolymeric nanoparticles: potential nanoplateforms for anti-cancer agent delivery. *Current Drug Targets*. 2011; 12: 1131–1150.
- [44] Repp L, Rasoulianboroujeni M, Lee HJ, Kwon GS. Acyl and oligo(lactic acid) prodrugs for PEG-b-PLA and PEG-b-PCL nano-assemblies for injection. *Journal of Controlled Release: Official Journal of the Controlled Release Society*. 2021; 330: 1004–1015.
- [45] Pang Z, Zhou J, Sun C. Ditelluride-Bridged PEG-PCL Copolymer as Folic Acid-Targeted and Redox-Responsive Nanoparticles for Enhanced Cancer Therapy. *Frontiers in Chemistry*. 2020; 8: 156.
- [46] Zhang D, Zou Z, Ren W, Qian H, Cheng Q, Ji L, *et al.* Gambogic acid-loaded PEG-PCL nanoparticles act as an effective antitumor agent against gastric cancer. *Pharmaceutical Development and Technology*. 2018; 23: 33–40.
- [47] Jin MJ, Piao SJ, Jin TX, Jin ZH, Yin XZ, Gao ZG. Improved anti-tumor efficiency against prostate cancer by docetaxel-loaded PEG-PCL micelles. *Journal of Huazhong University of Science and Technology. Medical Sciences*. 2014; 34: 66–75.
- [48] Cuong NV, Jiang JL, Li YL, Chen JR, Jwo SC, Hsieh MF. Doxorubicin-Loaded PEG-PCL-PEG Micelle Using Xenograft Model of Nude Mice: Effect of Multiple Administration of Micelle on the Suppression of Human Breast Cancer. *Cancers*. 2010; 3: 61–78.
- [49] Nguyen CT, Ann J, Sahu R, Byun WS, Lee S, Nam G, *et al.* Discovery of novel anti-breast cancer agents derived from deguelin as inhibitors of heat shock protein 90 (HSP90). *Bioorganic & Medicinal Chemistry Letters*. 2020; 30: 127374.
- [50] Kang W, Zheng X, Wang P, Guo S. Deguelin exerts anticancer activity of human gastric cancer MGC-803 and MKN-45 cells *in vitro*. *International Journal of Molecular Medicine*. 2018; 41: 3157–3166.
- [51] Li S, Wang Y, Zhao C, Zhang M, Wang W, Yu X, *et al.* Akt inhibitor deguelin aggravates inflammation and fibrosis in myocarditis. *Iranian Journal of Basic Medical Sciences*. 2019; 22: 1275–1282.
- [52] Ma J, Fang L, Yang Q, Hibberd S, Du WW, Wu N, *et al.* Post-transcriptional regulation of AKT by circular RNA angiomin-like 1 mediates chemoresistance against paclitaxel in breast cancer cells. *Aging*. 2019; 11: 11369–11381.
- [53] Li G, Xu D, Sun J, Zhao S, Zheng D. Paclitaxel inhibits proliferation and invasion and promotes apoptosis of breast cancer cells by blocking activation of the PI3K/AKT signaling pathway. *Advances in Clinical and Experimental Medicine: Official Organ Wroclaw Medical University*. 2020; 29: 1337–1345.
- [54] Lee SC, Min HY, Choi H, Bae SY, Park KH, Hyun SY, *et al.* Deguelin Analogue SH-1242 Inhibits Hsp90 Activity and Exerts Potent Anticancer Efficacy with Limited Neurotoxicity. *Cancer Research*. 2016; 76: 686–699.